

**Synthesis and Magnetic Studies of Pentagonal Bipyramidal
Metal Complexes of Fe, Co and Ni**

Journal:	<i>Dalton Transactions</i>
Manuscript ID	DT-ART-12-2018-005074.R1
Article Type:	Paper
Date Submitted by the Author:	06-Feb-2019
Complete List of Authors:	Deng, Yi-Fei; Southern University of Science and Technology, Chemistry Yao, Bin-Ling; Southern University of Science and Technology, Chemistry Zhan, Peng-Zhi; Southern University of Science and Technology, Chemistry Gan, De-Xuan; Southern University of Science and Technology, Chemistry Zhang, Yuan-Zhu; Southern University of Science and Technology, Chemistry Dunbar, Kim; Texas A&M University, Department of Chemistry



Journal Name

ARTICLE

Synthesis and Magnetic Studies of Pentagonal Bipyramidal Metal Complexes of Fe, Co and Ni

Yi-Fei Deng,^a Binling Yao,^a Peng-Zhi Zhan,^a Dexuan Gan,^a Yuan-Zhu Zhang^{*a} and Kim R. Dunbar^{*b}

Received 00th January 20xx,
Accepted 00th January 20xx

DOI: 10.1039/x0xx00000x

www.rsc.org/

Three mononuclear metal Complexes $[M(L-N_3O_2)(MeCN)_2][BPh_4]_2$ ($M = Fe, \mathbf{1}; Co, \mathbf{2}; Ni, \mathbf{3}$) were isolated and structurally characterized. Magnetic studies revealed uniaxial magnetic anisotropy for **1** ($D = -17.1 \text{ cm}^{-1}$) and **3** ($D = -14.3 \text{ cm}^{-1}$) and easy-plane magnetic anisotropy for **2** ($D = +36.9 \text{ cm}^{-1}$). Slow magnetic relaxation was observed for complexes **1** and **2** under an applied magnetic field, both of which are dominated by a Raman process.

Introduction

Mononuclear Single Molecule Magnets (SMMs) have attracted intense attention owing to their enhanced properties including higher blocking temperatures (T_B) and effective energy barriers (U_{eff})¹ that bode well for future applications in quantum computing and information storage devices.² The key issue in this area for designing SMMs is a fundamental understanding of the origin of magnetic anisotropy and dynamic relaxation in mononuclear complexes. Magnetic anisotropy achieved by strict regulation of geometry is the most critical factor for high-performance mononuclear SMMs,³ as indicated by reports of mononuclear lanthanide complexes beginning with the double-decker compounds $[Ln(III)PC_2]^-$ ($Ln = Tb, Dy$)⁴ to the very recent Dy(III) complexes with D_{5h} symmetry⁵, quasi-linear⁶ and metallocene structures.¹ For the 3d metal SMMs, fine-tuning of the magnetic anisotropy via coordination environment dictates the ligand field splitting which is paramount in contrast to lanthanide complexes for which magnetic anisotropy is more affected by the spin-orbit coupling (SOC).^{7,8} Important examples of 3d mononuclear SMMs include a series of Fe(I) and Co(II) complexes with linear,⁹ trigonal prismatic,¹⁰ and distorted tetrahedral coordination geometry,¹¹ which exhibit significant magnetic anisotropy and high effective energy barriers comparable to the lanthanide SMMs under zero or a small applied dc field. The success of research in transition metal mononuclear SMMs notwithstanding, it remains challenging to manipulate the ligand field and the molecular symmetry; one must also consider that nuclear hyperfine coupling and dipolar interactions can be dominant.¹²

Studies of mononuclear 3d mononuclear SMMs have revealed that magnetic anisotropy mainly originates from the mixing of the ground state and the excited state through SOC, which is usually quenched or diminished due to the large ligand-field splitting energies of d orbitals. This issue can be circumvented in low coordination number complexes with a relatively weak ligand field which leads to d orbitals in a narrow energy range. In such cases, there are stronger interactions between the ground and excited states and thus larger magnetic anisotropy.¹³ As a result, a variety of coordinatively unsaturated 3d complexes with coordination numbers ranging from 2-6 have been investigated and found to exhibit slow relaxation of the magnetization.¹⁴ Nevertheless, theoretical predictions support the contention that higher-coordinate mononuclear 3d metal complexes are also capable of exhibiting large magnetic anisotropy.¹⁵ Indeed, a few mononuclear Fe(II) and Co(II) complexes with pentagonal bipyramidal geometries¹⁶ and the subsequent Ising chains¹⁷ constructed from such units were investigated with the results indicating considerable magnetic anisotropy and slow magnetic relaxation.

In prior work from our laboratories, we reported the Fe(II)-based cyanide-bridged single molecule magnet $[Cr^{III}Fe^{II}_2]$ with an energy barrier of 44.3 K which is among the best cyanide SMMs to date. In this compound the Fe(II) is in a pentagonal bipyramidal geometry enforced by an azaoxa-macrocycle ligand of $L-N_3O_2$.¹⁸ This result supports the contention that Fe(II) ion in a pentagonal bipyramidal geometry can exhibit large uniaxial anisotropy. Herein we report the results of a systematic magnetic study of three pentagonal bipyramidal complexes $[M(L-N_3O_2)(MeCN)_2][BPh_4]_2$ ($M = Fe, \mathbf{1}; Co, \mathbf{2}; Ni, \mathbf{3}$; $L-N_3O_2 = 2,13$ -dimethyl-6,9-dioxa-3,12,18-triazabicyclo-[12.3.1]octadeca-1(18),2,12,14,16-pentaene). Magnetic studies revealed uniaxial magnetic anisotropy for complexes **1** and **3** and easy-plane magnetic anisotropy for **2**. Dynamic magnetic measurements revealed slow relaxation of the magnetization for **1** and **2**.

^a Department of Chemistry, Southern University of Science and Technology, Shenzhen, 518055, P. R. China
E-mail: zhangyz@sustc.edu.cn

^b Department of Chemistry, Texas A & M University, College Station, TX 77842, USA
E-mail: dunbar@chem.tamu.edu

† Electronic Supplementary Information (ESI) available. CCDC 1861079-1861081. For ESI and crystallographic data in CIF or other electronic format see DOI: 10.1039/x0xx00000x.

Experimental Section

Materials and Physical Measurements.

All chemicals were commercially available and used as received. Compound **1** was performed under a dry and oxygen-free argon atmosphere by using Schlenk techniques or in a glovebox. Complexes **2** and **3** were synthesized in air. Powder X-ray Diffraction (PXRD) measurements were recorded on a Rigaku Smartlab X-ray diffractometer and the experimental patterns matched well with the simulated one, indicating that the samples are pure (Figure S4). Direct-current (dc, 2-300K, 0-7 T) and alternating-current (ac, at frequencies between 1 and 1500 Hz with an ac field of 5 Oe) susceptibility measurements were performed on powder samples of **1-3** with a Quantum Design MPMS XL-7 SQUID magnetometer. Diamagnetic corrections were calculated from Pascal constants¹⁹ and applied to all the constituent atoms and the sample holder. All SQUID samples were immobilized in the capsule with eicosane to avoid magnetic torqueing. Multiconfigurational *ab initio* calculations were performed using the ORCA 3.0.3 computational package.²⁰ The polarized triple- ζ -quality basis set [def2-TZVPP] proposed by Ahlrichs and co-workers was used for Fe, Co and Ni ions; def2-TZVP was used for nitrogen and oxygen atoms, while the basis set def2-SVP was used for other remote atoms.²¹

General procedure for the synthesis of $[M^{II}(L-N_3O_2)(H_2O)_2][ClO_4]_2$ and $[M^{II}(L-N_3O_2)(MeCN)_2][BPh_4]_2$ ($M = Fe, \mathbf{1}; Co, \mathbf{2}; Ni, \mathbf{3}$)

$[M^{II}(L-N_3O_2)(H_2O)_2][ClO_4]_2$: 2,6-Diacetylpyridine (16 mg, 0.1 mmol) and 1,8-Diamino-3,6-dioxaoctane (15.0 mg, 0.10 mmol) were added to a MeOH/H₂O (10 mL, 2:1) solution of $Fe(ClO_4)_2 \cdot (H_2O)_5$ (25 mg, 0.10 mmol). The mixture was refluxed for 12 h and filtrated after cooling to room temperature. Then the mixture was filtrated and the filtrate was concentrated and cooled at 4 °C to obtain the crystals, which was collected and dried under vacuum; yield 52%. The Co(II) and Ni(II) analogues were obtained in a similar way (Yield: 50-60%) using the $Co(ClO_4)_2 \cdot (H_2O)_6$ and $Ni(ClO_4)_2 \cdot (H_2O)_6$ instead.

$[M^{II}(L-N_3O_2)(MeCN)_2][BPh_4]_2$: To a solution of $[Fe(L-N_3O_2)(H_2O)_2][ClO_4]_2$ (227 mg, 0.10 mmol) in acetonitrile (10 mL) was slowly added an acetonitrile (5 mL) solution of sodium tetraphenylborate (69 mg, 0.20 mmol). The resulting mixture was filtered and the filtrate was left to stand undisturbed for two weeks. Single crystals were collected and dried under vacuum; yield 67%. Complexes **2** and **3** (Yield: 60-70%) were obtained in a similar manner with the corresponding metal precursors.

Crystallography

X-ray data for **1-3** were collected at 110(2) K on a Bruker D8 VENTURE diffractometer with graphite monochromated Mo K α radiation ($\lambda = 0.71073 \text{ \AA}$). Lorentz/polarization corrections were applied during data reduction and the structures were solved by direct methods (SHELXS-97). Refinements were performed by full-matrix least squares (SHELXL-97)²² on F^2 and empirical absorption corrections (SADABS)²³ were applied. Anisotropic thermal parameters were used for the non-hydrogen atoms. Hydrogen atoms were added at calculated positions and refined using a riding model. Weighted R factors (wR) and the goodness-of-fit (S) values are based on F^2 ; conventional R factors (R) are based on F , with F set to zero for negative F^2 . Data

collection and structural refinement parameters are provided in Table 1 and selected bond distances and angles are listed in Table S1. CCDC-1861079-1861081 contain the crystallographic data that can be obtained via www.ccdc.cam.ac.uk/conts/retrieving.html (or from the Cambridge Crystallographic Data Centre, 12, Union Road, Cambridge CB21EZ, UK; fax: (+44) 1223-336-033; or deposit@ccdc.cam.ac.uk).

Results and discussion

Synthesis and Structure Characterization

The air-stable compounds **1-3** were easily prepared by the reaction of the precursor salt $[M(L-N_3O_2)(H_2O)_2][ClO_4]_2$ with sodium tetraphenylborate in acetonitrile solution.

Table 1. X-ray crystallographic data for complexes **1-3**.

	1	2	3
Empirical formula	C ₆₇ H ₆₇ B ₂ FeN ₅ O ₂	C ₆₇ H ₆₇ B ₂ CoN ₅ O ₂	C ₆₇ H ₆₇ B ₂ NiN ₅ O ₂
Formula weight/g mol ⁻¹	1051.72	1054.80	1054.58
crystal system	Orthorhombic	Orthorhombic	Orthorhombic
space group	<i>Pbcn</i>	<i>Pbcn</i>	<i>Pbcn</i>
<i>a</i> , Å	16.397(3)	16.401(6)	16.409(10)
<i>b</i> , Å	19.194(4)	19.168(7)	19.183(11)
<i>c</i> , Å	17.667(4)	17.676(7)	17.634(10)
α , deg	90	90	90
β , deg	90	90	90
γ , deg	90	90	90
<i>V</i> , Å ³	5560(2)	5557(4)	5551(6)
<i>Z</i>	4	4	4
$d_{cal} / g \text{ cm}^{-3}$	1.256	1.261	1.262
$F(000)$	2224	2228	2232
Temperature, K	110(2)	110(2)	110(2)
Radiation	MoK α	MoK α	MoK α
ϑ range	3.42–25°	1.63–26.18°	1.63–25.17°
completeness	99.6%	99.6%	99.3%
residual map, e Å ⁻³	0.93/-0.35	0.38/-0.46	0.39/-0.48
Goodness-of-fit on F^2	1.039	1.029	1.028
R indices [$>2\sigma(I)$]	$R_1 = 0.0571$, $wR_2 = 0.1312$	$R_1 = 0.0385$, $wR_2 = 0.0925$	$R_1 = 0.0521$, $wR_2 = 0.1054$
R indices (all data)	$R_1 = 0.0812$, $wR_2 = 0.1491$	$R_1 = 0.0539$, $wR_2 = 0.1024$	$R_1 = 0.0950$, $wR_2 = 0.1275$

All of the complexes **1-3** crystallize in the orthorhombic space group *Pbcn* (Figures 1, S1-S3). The central metal ion is situated in a pentagonal bipyramidal coordination sphere formed by five equatorial N3O2 (N1, N2, N2A, O1, O1A) atoms from the ligands and two axial N atoms (N3, N3A) from the MeCN molecules. The axial bond angles for **1** and **2** are $\sim 173^\circ$ (N3-Fe-N3A, 172.25(14)°; N3-Co-N3A, 173.21(8)°), whereas the smaller angle N3-Ni-N3A of 169.26(15)° was found in complex **3**. The equatorial M-O bond lengths of complexes **1-3** are significantly longer than the M-N bond distances (Table S1). All the equatorial N-M-O(N) bond angles of complexes **1** and **2** are in the narrow range of $\sim 73^\circ$ (**1**, 72.02(9)-73.03(7)°; **2**, 72.46(6)-72.70(4)°). The corresponding angles for **3** vary

from 70.96(10) to 77.06(8)°, an indication of a more distorted pentagonal bipyramidal geometry for **3**. The SHAPE software²⁴ gave the deviation parameters of 0.137, 0.129, and 0.477 for **1-3** respectively, which are close to zero of the ideal D_{5h} symmetry while the larger value for **3** confirms the more distortion. Due to the large size of the tetraphenylborate anion, the metal centers are well isolated with the closest intermolecular metal...metal separations being 11.5, 11.5, 11.7 Å for **1-3**, respectively (Figures S1-S3).

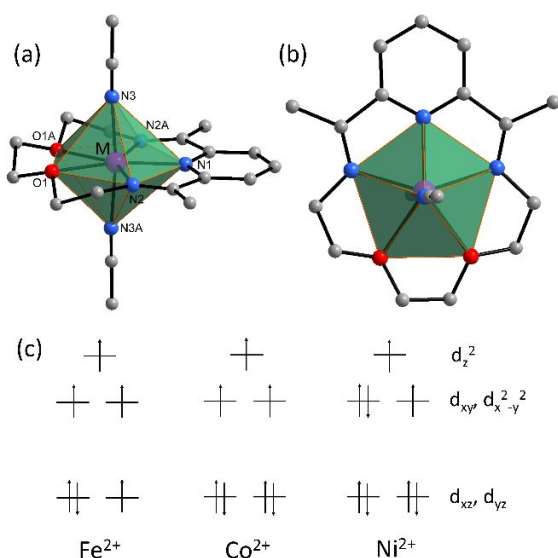


Figure 1. Structure of the pentagonal bipyramidal complexes ($M = \text{Fe}, \text{Co}, \text{Ni}$) viewed from the side (a) and the top (b) (H atoms and counter anions were omitted for clarity); (c) The electron configuration of $\text{Fe}(\text{II})$, $\text{Co}(\text{II})$, $\text{Ni}(\text{II})$ in pentagonal bipyramidal geometry.

Magnetic Properties

Variable temperature dc susceptibility measurements were performed on powder samples at a dc field of 1000 Oe (Figure 2). The $\chi_M T$ product at room temperature is 3.85, 2.12 and 1.03 $\text{cm}^3 \text{K mol}^{-1}$ for **1-3**, respectively, larger than the calculated values for the spin-only contributions, indicating considerable contribution from orbital angular momentum.²⁵ Upon cooling, $\chi_M T$ values are essentially

constant, decreasing at about 40 K (for **1**), 60 K (for **2**) and 15 K (for **3**) which is likely attributed to the magnetic anisotropy of the metal ions. The field-dependent magnetization data for **1-3** were measured from 0 to 7 T from 2-6 K. All of the complexes exhibited continuously increases to 2.79, 1.98 and 1.49 $\text{N}\beta$ for **1-3** at 7 T and 2 K, respectively. The lack of high-field saturation suggests the presence of significant magnetic anisotropy. In order to gain insight into the magnetic anisotropy, the PHI program²⁶ was employed to analyze the dc susceptibility data and magnetization data, wherein $\chi_M T$ vs T and M - H data were fitted simultaneously based with the following spin Hamiltonian (eqn. 1, with $g_x = g_y$):

$$\hat{H} = D(\hat{S}_z^2 - S(S+1)/3) + E(\hat{S}_x^2 - \hat{S}_y^2) + \mu_B \sum_{i=x,y,z} \hat{S}_i g_i B_i$$

where E is the rhombic ZFS parameter, μ_B is the Bohr magneton, g is the Landé factor and B is the magnetic induction. The best fit was achieved with parameters: **1**: $g_x = g_y = 2.16$, $g_z = 2.42$, $D = -17.1 \text{ cm}^{-1}$, $E = \pm 0.6 \text{ cm}^{-1}$, $R = 1.3 \times 10^{-4}$; **2**: $g_x = g_y = 2.18$, $g_z = 2.01$, $D = +36.9 \text{ cm}^{-1}$, $E = \pm 0.2 \text{ cm}^{-1}$, $R = 4.3 \times 10^{-5}$; **3**: $g_x = g_y = 1.79$, $g_z = 2.39$, $D = -14.3 \text{ cm}^{-1}$, $E = \pm 1.8 \text{ cm}^{-1}$, $R = 5.2 \times 10^{-5}$. The results of D , E , and g values are well in consistent with the previous reported mononuclear complexes with similar coordination geometries. And imposing an opposite initial D value would result in a poor fit, which is also conflict with the reported EPR data and theoretical calculations for similar complexes, indicating that magnetic fitting should be reliable.¹⁶ In order to further explore the magnetic anisotropy of the complexes, multi-configurational *ab initio* CASSCF/NEVPT2 calculations were performed on the experimental structures (Table S3 and S4). In the case of spin Hamiltonian parameters of $S = 3/2$, the calculated axial zero-field splitting (zfs) parameter D is -19.7 cm^{-1} , $+37.8 \text{ cm}^{-1}$ and -15.4 cm^{-1} for complexes **1-3**, respectively. Both the calculated axial zfs parameter (D) and rhombic ZFS parameter (E) agree well with the experiment values and further confirm the uniaxial magnetic anisotropy for **1** and **3** while easy plane magnetic anisotropy for **2**. The result is also well in the agreement with those previous reports for this special geometry.¹⁶

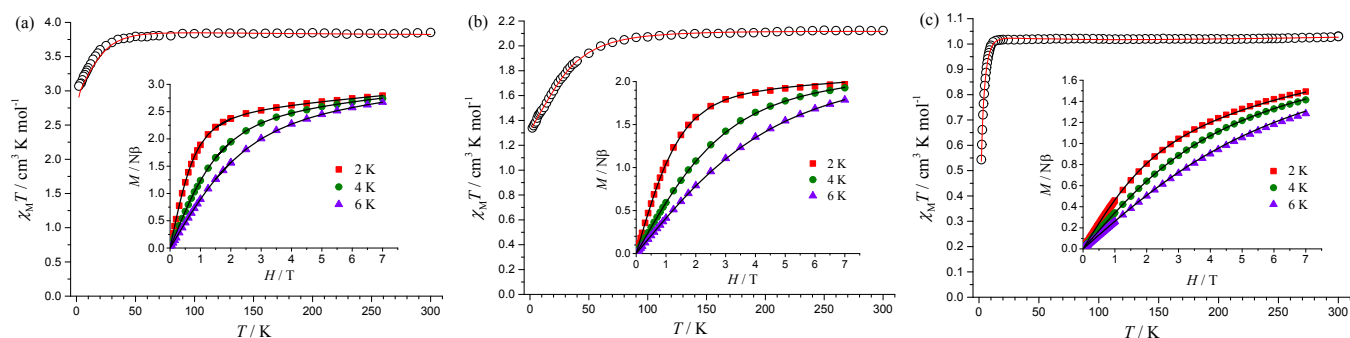


Figure 2. Temperature dependence of $\chi_M T$ obtained at 1000 Oe (data points) for **1**(a), **2**(b) and **3**(c). Solid lines represent the fits with the PHI program. Inset shows the 2-6 K field-dependent magnetization and its fit obtained simultaneously with the $\chi_M T$ fit.

Dynamic magnetic measurements were measured to probe the SMM behavior of **1-3** (Figure 3, Figures S5-S9). Under zero dc field, no slow magnetic relaxation was observed for all the complexes, while frequency-dependent behavior with obvious

out-of-phase ac susceptibility (χ'') signals appeared when a small dc field was applied for complexes **1** and **2**, typical of 3d SMMs with fast quantum tunnelling of the magnetization (QTM).²⁷ However, no SMM behavior was observed for **3** even

with the field up to 7000 Oe. Studies of the reported mononuclear Ni(II) complexes indicated that only a few Ni(II) examples exhibit moderate SMM behaviour even with huge magnetic anisotropy,²⁸ due to the efficient quantum tunnelling of the magnetization. We believe that a more distorted pentagonal bipyramidal geometry of complex **3** would contribute to a dominant QTM effect and thus the absence of SMM behaviour.

The Cole–Cole plots for **1** and **2** at different temperatures were fitted with the generalized Debye model²⁹ (Figure S8), yielding the relaxation time (τ) as well as the distribution coefficients α (Table S2). The relaxation times τ were plotted versus T^{-1} , generating the Arrhenius-like diagram. Both the Arrhenius diagrams were temperature-dependent and barely linear in the high-temperature region, yielding an estimation of the energy barrier of 50(2) K and 32(1) K, respectively (Figure 3). Both values are much less than the Orbach-only energy barrier as evaluated from the D value, indicating other “shortcut” paths for the relaxation of magnetization. The general model containing four relaxation processes (QTM, direct, Raman and Orbach process) should be employed for analysis while this would lead to overparameterized fit results. In order to avoid the overparameterization, both the direct and QTM processes were neglected for complex **1** since they were negligible under the small optimum field (eqn. 2)³⁰:

$$\tau^{-1} = CT^n + \tau_0^{-1} \exp(-U/k_B T)$$

Where C and n – coefficients, T – temperature, U – energy barrier, τ_0 – pre-exponential factor, k_B – Boltzmann constant. The best fit was obtained giving $C = 131(9) \text{ K}^{-2.1} \text{ s}^{-1}$, $\tau_0 = 3.4(2) \times 10^{-11} \text{ s}^{-1}$, $U/k_B = 89(2) \text{ K}$, $n = 2.1(1)$. For the overall process, the Raman relaxation prevails at most temperatures, whereas the Orbach pathway becomes important at the higher temperatures. Nevertheless, the Raman process still has a significant effect on the overall relaxation properties, therefore the energy barrier obtained from the high-temperature region ($U_{\text{eff}} = 50 \text{ K}$) is much lower than the calculated barrier for an Orbach process only ($U = 98 \text{ K}$).

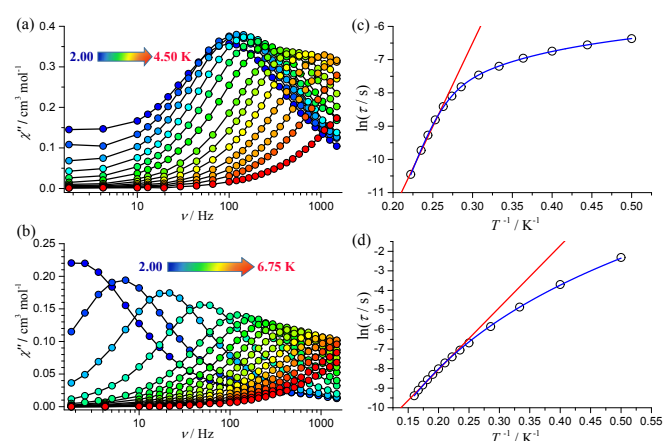


Figure 3. Frequency dependent magnetic susceptibilities of the out-of-phase signals for **1**(a) and **2**(b) at indicated dc field; the lines are guides to the eyes. Temperature dependence of the relaxation rates for **1**(c) and **2**(d). The red lines correspond to the high-temperature Arrhenius fitting. The blue lines represent the fitting based on eqn. 2.

As for complex **2** with easy plane magnetic anisotropy, generally there are three potential reasons for the occurrence of slow

relaxation, including a field-induced bottleneck effect,^{31a} the presence of the large rhombic anisotropy barrier determined by the E parameter^{31b} and a dominant optical acoustic Raman process^{31c}. In this case, both the first two reasons were excluded due to the small effective energy barrier and small experimental E value, which seems that the magnetic relaxation would proceed more likely through the optical acoustic Raman process involving a virtual state. During the fitting of **2**, we found that the relaxation times can be fitted well to a T^{-n} law with $C = 0.15(2) \text{ K}^{-6.2} \text{ s}^{-1}$ and $n = 6.2(3)$ (Figure S9), indicating that a dominant optical acoustic Raman process³² is responsible for the spin relaxation observed in **2**.

Conclusions

In summary, we have examined three mononuclear metal(II) complexes ($M = \text{Fe, Co, Ni}$) with the pentagonal bipyramidal geometry. Both complexes **1** and **3** exhibit uniaxial magnetic anisotropy and complex **2** exhibits easy-plane magnetic anisotropy. Dynamic magnetic measurements reveal slow relaxation of magnetization for **1** and **2**, both of which involve considerable contribution from Raman processes. It is noted that the magnetic anisotropy and relaxation dynamics are very sensitive to small changes in ligand field and/or the central metal ions in this coordination geometry. Additional studies of magneto-structural correlations for such modified complexes are in progress.

Acknowledgements

This work was supported by the National Natural Science Foundation of China (No. 21671095), Thousand Talents Program-Youth, and start-up fund from SUSTech. KRD gratefully acknowledges the National Science Foundation (CHE-1808779) and the Robert A. Welch Foundation (A-1449).

Notes and references

- (a) C. A. P. Goodwin, F. Ortu, D. Reta, N. F. Chilton and D. P. Mills, *Nature*, 2017, **548**, 439; (b) F.-S. Guo, B. M. Day, Y.-C. Chen, M.-L. Tong, A. Mansikkamäki and R. A. Layfield, *Angew. Chem., Int. Ed.*, 2017, **56**, 11445-11449; (c) F.-S. Guo, B. M. Day, Y.-C. Chen, M.-L. Tong, A. Mansikkamäki and R. A. Layfield, *Science*, 2018, DOI: 10.1126/science.aav0652; (d) K. R. McClain, C. A. Gould, K. Chakarawet, S. Teat, T. J. Groshens, J. R. Long and B. G. Harvey, *Chem. Sci.*, 2019, DOI: 10.1039/c8sc03907k.
- (a) C. Cervetti, A. Rettori, M. G. Pini, A. Cornia, A. Repollés, F. Luis, M. Dressel, S. Rauschenbach, K. Kern, M. Burghard and L. Bogani, *Nat. Mater.*, 2015, **15**, 164; (b) M. Shiddiq, D. Komijani, Y. Duan, A. Gaita-Ariño, E. Coronado and S. Hill, *Nature*, 2016, **531**, 348; (c) Z. Hu, B.-W. Dong, Z. Liu, J.-J. Liu, J. Su, C. Yu, J. Xiong, D.-E. Shi, Y. Wang, B.-W. Wang, A. Ardavan, Z. Shi, S.-D. Jiang and S. Gao, *J. Am. Chem. Soc.*, 2018, **140**, 1123-1130; (d) Y.-X. Wang, Y. Ma, Y. Chai, W. Shi, Y. Sun and P. Cheng, *J. Am. Chem. Soc.*, 2018, **140**, 7795-7798.
- (a) D. N. Woodruff, R. E. P. Winpenny and R. A. Layfield, *Chem. Rev.*, 2013, **113**, 5110-5148; (b) L. Ungur and L. F. Chibotaru, *Inorg. Chem.*, 2016, **55**, 10043-10056; (c) A. K. Bar, C. Pichon and J.-P. Sutter, *Coord. Chem. Rev.*, 2016, **308**, 346-380.
- (a) N. Ishikawa, M. Sugita, T. Ishikawa, S.-y. Koshihara and Y. Kaizu, *J. Am. Chem. Soc.*, 2003, **125**, 8694-8695.

5. (a) J. Liu, Y.-C. Chen, J.-L. Liu, V. Vieru, L. Ungur, J.-H. Jia, L. F. Chibotaru, Y. Lan, W. Wernsdorfer, S. Gao, X.-M. Chen and M.-L. Tong, *J. Am. Chem. Soc.*, 2016, **138**, 5441-5450; (b) Y.-C. Chen, J.-L. Liu, L. Ungur, J. Liu, Q.-W. Li, L.-F. Wang, Z.-P. Ni, L. F. Chibotaru, X.-M. Chen and M.-L. Tong, *J. Am. Chem. Soc.*, 2016, **138**, 2829-2837; (c) Y.-S. Ding, N. F. Chilton, R. E. P. Winpenny and Y.-Z. Zheng, *Angew. Chem., Int. Ed.*, 2016, **55**, 16071-16074; (d) S. K. Gupta, T. Rajeshkumar, G. Rajaraman and R. Murugavel, *Chem. Sci.*, 2016, **7**, 5181-5191.
6. (a) N. F. Chilton, C. A. P. Goodwin, D. P. Mills and R. E. P. Winpenny, *Chem. Commun.*, 2015, **51**, 101-103; (b) Y.-S. Meng, L. Xu, J. Xiong, Q. Yuan, T. Liu, B.-W. Wang and S. Gao, *Angew. Chem., Int. Ed.*, 2018, **57**, 4673-4676.
7. L. F. Chibotaru, *Struct. Bond*, 2015, **164**, 185-229.
8. B. N. Figgis, M. A. Hitchman, *Ligand field theory and its applications*. Wiley-VCH, New York, 1999.
9. (a) J. M. Zadrozny, D. J. Xiao, M. Atanasov, G. J. Long, F. Grandjean, F. Neese and J. R. Long, *Nat. Chem.*, 2013, **5**, 577; (b) X.-N. Yao, J.-Z. Du, Y.-Q. Zhang, X.-B. Leng, M.-W. Yang, S.-D. Jiang, Z.-X. Wang, Z.-W. Ouyang, L. Deng, B.-W. Wang and S. Gao, *J. Am. Chem. Soc.*, 2017, **139**, 373-380.
10. (a) Y.-Y. Zhu, C. Cui, Y.-Q. Zhang, J.-H. Jia, X. Guo, C. Gao, K. Qian, S.-D. Jiang, B.-W. Wang, Z.-M. Wang and S. Gao, *Chem. Sci.*, 2013, **4**, 1802-1806; (b) V. V. Novikov, A. A. Pavlov, Y. V. Nelyubina, M.-E. Boulon, O. A. Varzatskii, Y. Z. Voloshin and R. E. P. Winpenny, *J. Am. Chem. Soc.*, 2015, **137**, 9792-9795.
11. (a) J. M. Zadrozny and J. R. Long, *J. Am. Chem. Soc.*, 2011, **133**, 20732-20734; (b) E. Carl, S. Demeshko, F. Meyer and D. Stalke, *Chem. Eur. J.*, 2015, **21**, 10109-10115; (c) Y. Rechkemmer, F. D. Breitgoff, M. van der Meer, M. Atanasov, M. Hakl, M. Orlita, P. Neugebauer, F. Neese, B. Sarkar and J. van Slageren, *Nat. Commun.*, 2016, **7**, 10467.
12. (a) S. Gómez-Coca, A. Urtizberea, E. Cremades, P. J. Alonso, A. Camón, E. Ruiz and F. Luis, *Nat. Commun.*, 2014, **5**, 4300; (b) T. J. Woods, M. F. Ballesteros-Rivas, S. Gómez-Coca, E. Ruiz and K. R. Dunbar, *J. Am. Chem. Soc.*, 2016, **138**, 16407-16416.
13. (a) P. P. Power, *Chem. Rev.*, 2012, **112**, 3482-3507; (b) M. Dey and N. Gogoi, *Angew. Chem., Int. Ed.*, 2013, **52**, 12780-12782.
14. (a) D. E. Freedman, W. H. Harman, T. D. Harris, G. J. Long, C. J. Chang and J. R. Long, *J. Am. Chem. Soc.*, 2010, **132**, 1224-1225; (b) J. Vallejo, I. Castro, R. Ruiz-García, J. Cano, M. Julve, F. Lloret, G. De Munno, W. Wernsdorfer and E. Pardo, *J. Am. Chem. Soc.*, 2012, **134**, 15704-15707; (c) R. C. Poulten, M. J. Page, A. G. Algarra, J. J. Le Roy, I. López, E. Carter, A. Lobet, S. A. Macgregor, M. F. Mahon, D. M. Murphy, M. Murugesu and M. K. Whittlesey, *J. Am. Chem. Soc.*, 2013, **135**, 13640-13643; (d) Y.-F. Deng, T. Han, Z. Wang, Z. Ouyang, B. Yin, Z. Zheng, J. Krzystek and Y.-Z. Zheng, *Chem. Commun.*, 2015, **51**, 17688-17691; (e) J. M. Frost, K. L. M. Harriman and M. Murugesu, *Chem. Sci.*, 2016, **7**, 2470-2491.
15. (a) R. Ruamps, L. J. Batchelor, R. Maurice, N. Gogoi, P. Jiménez-Lozano, N. Guihéry, C. deGraaf, A.-L. Barra, J.-P. Sutter and T. Mallah, *Chem. Eur. J.*, 2013, **19**, 950-956; (b) S. Gomez-Coca, E. Cremades, N. Aliaga-Alcalde and E. Ruiz, *J. Am. Chem. Soc.*, 2013, **135**, 7010-7018.
16. (a) T. S. Venkatakrishnan, S. Sahoo, N. Bréfuel, C. Duhayon, C. Paulsen, A.-L. Barra, S. Ramasesha and J.-P. Sutter, *J. Am. Chem. Soc.*, 2010, **132**, 6047-6056; (b) X.-C. Huang, C. Zhou, D. Shao and X.-Y. Wang, *Inorg. Chem.*, 2014, **53**, 12671-12673; (c) L. Chen, S.-Y. Chen, Y.-C. Sun, Y.-M. Guo, L. Yu, X.-T. Chen, Z. Wang, Z. W. Ouyang, Y. Song and Z.-L. Xue, *Dalton. Trans.*, 2015, **44**, 11482-11490; (d) D. Shao, X.-H. Zhao, S.-L. Zhang, D.-Q. Wu, X.-Q. Wei and X.-Y. Wang, *Inorg. Chem. Front.*, 2015, **2**, 846-853; (e) D. Shao, S.-L. Zhang, L. Shi, Y.-Q. Zhang and X.-Y. Wang, *Inorg. Chem.*, 2016, **55**, 10859-10869; (f) H. Lou, L. Yin, B. Zhang, Z.-W. Ouyang, B. Li and Z. Wang, *Inorg. Chem.*, 2018, **57**, 7757-7762; (g) C. Pichon, N. Suaud, C. Duhayon, N. Guihéry and J.-P. Sutter, *J. Am. Chem. Soc.*, 2018, **140**, 7698-7704.
17. (a) L. J. Batchelor, M. Sangalli, R. Guillot, N. Guihéry, R. Maurice, F. Tuna and T. Mallah, *Inorg. Chem.*, 2011, **50**, 12045-12052; (b) N. Gogoi, M. Thlijeni, C. Duhayon and J.-P. Sutter, *Inorg. Chem.*, 2013, **52**, 2283-2285; (c) A. K. Bar, C. Pichon, N. Gogoi, C. Duhayon, S. Ramasesha and J.-P. Sutter, *Chem. Commun.*, 2015, **51**, 3616-3619; (d) A. K. Bar, N. Gogoi, C. Pichon, V. M. Goli, M. Thlijeni, C. Duhayon, N. Suaud, N. Guihéry, A. L. Barra, S. Ramasesha and J. P. Sutter, *Chem. Eur. J.*, 2017, **23**, 4380-4396.
18. (a) Y.-Z. Zhang, B.-W. Wang, O. Sato and S. Gao, *Chem. Commun.*, 2010, **46**, 6959-6961.
19. G. A. Bain and J. F. Berry, *J. Chem. Educ.*, 2008, **85**, 532-536.
20. (a) F. Neese. *Wiley Interdiscip. Rev. Comput. Mol. Sci.*, 2012, **2**, 73; (b) F. Neese and F. Wennmohs. ORCA (v. 3.0.3), Stiftstr. 2013, 34-36.
21. (a) F. Weigend and R. Ahlrichs, *Phys. Chem. Chem. Phys.*, 2005, **7**, 3297; (b) A. Schafer, C. Huber and R. Ahlrichs. *J. Chem. Phys.*, 1994, **100**, 5829.
22. *SHELXTL 6.10*, Bruker Analytical Instrumentation, Madison, Wisconsin, USA, 2000.
23. G. M. Sheldrick. *SADABS 2.05*, University Göttingen, Germany, 2002.
24. *SHAPE, version 2.0; continuous shape measures calculation; Electronic Structure Group*. Universitat de Barcelona: Barcelona, Spain, 2010.
25. F. E. Mabbs and D. J. Machin, *Magnetism and Transition Metal Complexes*, Dover Publications: Mineola, NY, 2008.
26. N. F. Chilton, R. P. Anderson, L. D. Turner, A. Soncini and K. S. Murray, *J. Comput. Chem.*, 2013, **34**, 1164-1175.
27. D. Gatteschi and R. Sessoli, *Angew. Chem., Int. Ed.*, 2003, **42**, 268-297.
28. (a) J. Miklovič, D. Valigura, R. Boča and J. Titiš, *Dalton. Trans.*, 2015, **44**, 12484-12487; (b) K. E. R. Marriott, L. Bhaskaran, C. Wilson, M. Medarde, S. T. Ochsenbein, S. Hill and M. Murrie, *Chem. Sci.*, 2015, **6**, 6823-6828.
29. D. Gatteschi, R. Sessoli and R. Villain, *Molecular Nanomagnets.*, Oxford University Press, 2006.
30. R. L. Carlin and A. J. v. Duijneveldt, *Magnetic Properties of Transition Metal compounds*, Springer-Verlag, New York, 1976.
31. (a) J. M. Zadrozny, J. Liu, N. A. Piro, C. J. Chang, S. Hill and J. R. Long, *Chem. Commun.*, 2012, **48**, 3927-3929; (b) J. Vallejo, I. Castro, R. Ruiz-García, J. Cano, M. Julve, F. Lloret, G. De Munno, W. Wernsdorfer and E. Pardo, *J. Am. Chem. Soc.*, 2012, **134**, 15704-15707; (c) E. Colacio, J. Ruiz, E. Ruiz, E. Cremades, J. Krzystek, S. Carretta, J. Cano, T. Guidi, W. Wernsdorfer and E. K. Brechin, *Angew. Chem., Int. Ed.*, 2013, **52**, 9130-9134.
32. (a) K. N. Shrivastava, *Phys. status. solidi. B.*, 1983, **117**, 437-458.